Mendeleev Communications

Mendeleev Commun., 2025, **35**, 589–591

Fullerene C_{60} conjugated with L- and D-alanine: integration into lipid bilayer and protection of cell membrane against oxidative stress

Vladimir A. Volkov,*[a] Mikhail V. Voronkov,[a] Yakov N. Uglov,[b] Polina K. Gifer,[c] Valentina S. Romanova,[d] Vyacheslav M. Misin[a] and Oleg V. Batishchev[c]

[a] *N. M. Emanuel Institute of Biochemical Physics, Russian Academy of Sciences, 119334 Moscow, Russian Federation. Fax: +7 499 137 4101; e-mail: vl.volkov@mail.ru*
[b] *D. I. Mendeleev University of Chemical Technology of Russia, 125047 Moscow, Russian Federation*
[c] *A. N. Frumkin Institute of Physical Chemistry and Electrochemistry, Russian Academy of Sciences, 119071 Moscow, Russian Federation*
[d] *A. N. Nesmeyanov Institute of Organoelement Compounds, Russian Academy of Sciences, 119334 Moscow, Russian Federation*

DOI: 10.71267/mencom.7774

Using atomic force microscopy and a fluorescent probe, it was demonstrated that nanoparticles of *N*-(monohydrofullerenyl) alanine enantiomers effectively embedded into lipid membranes, reduce membrane microviscosity and increase membrane fluidity. Even at a concentration of 1 nM, these C_{60} fullerene derivatives were found to protect human erythrocytes from free radical-induced hemolysis. The particle sizes of the investigated compounds determined by atomic force microscopy are consistent with small-angle X-ray scattering data indicating the presence of stable aggregate configurations showing a two-fold difference between adjacent maxima in the radius distribution.

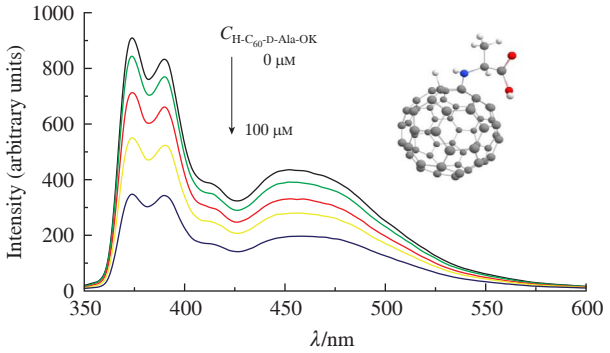

Keywords: fullerene, C_{60}, nanoparticles, lipid peroxidation, membrane fluidity, hemolysis, AFM, fluorescence, pyrene.

Since almost all biochemical processes in a living cell are associated with its membrane structures, interaction with the cell membrane is a critical aspect of the action of biologically active compounds. In the context of oxidative stress, a shift in the prooxidant–antioxidant balance disrupts the integrity and functionality of cellular membrane structures. From the perspective of regulating lipid peroxidation, antioxidants that can integrate into the lipid bilayer of cell membranes are of particular interest. The mechanism of their action may involve not only breaking of oxidation chains or the prevention of their initiation, but also the reduction of membrane microviscosity. In addition, the activity of many compounds capable of generating reactive oxygen species (ROS) increases in a lipid environment.[1] The reason is that inside the lipid membrane they have access to a pool of molecular oxygen, which is stored predominantly in the hydrophobic core of cell membranes.[2] Derivatives of fullerene C_{60} are a class of compounds exhibiting high antiradical and antioxidant activity.[3–10] Therefore, it is a pressing issue to investigate their interaction with lipid membranes and antioxidant activity in such an environment.

We have previously studied the structural parameters of *N*-monosubstituted amino acid fullerene C_{60} derivatives (AAFDs)† using dynamic light scattering and small-angle X-ray scattering (SAXS) methods.[11] Here, these results were confirmed and visualized (Figure 1) using atomic force microscopy (AFM).†

The particle size of the L-alanine derivative (H-C_{60}-L-Ala-OK) determined by AFM scanning in the working buffer (pH 7.0) ranges from 2.5 to 8.5 nm. The majority of the particles have a size of 3.6±0.6 nm, while the second maximum in the distribution is observed at approximately 6.9±0.9 nm. These results are consistent with the SAXS data, which indicate the presence of stable configurations of amino acid-derived fullerene aggregates,

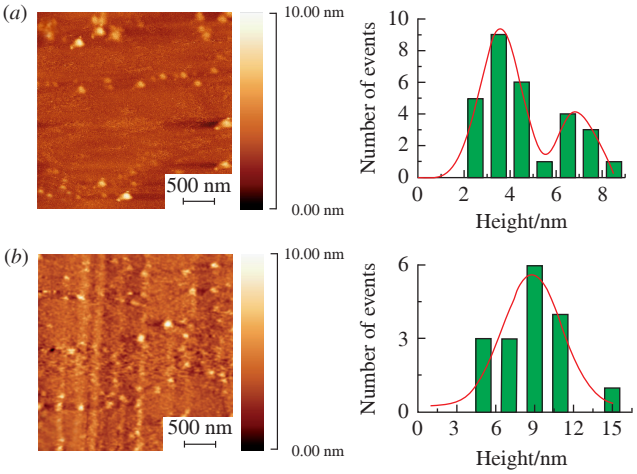

Figure 1 AFM images and particle size distribution curves of (*a*) H-C_{60}-L-Ala-OK and (*b*) H-C_{60}-D-Ala-OK nanoparticles deposited on freshly cleaved mica.

† For details, see Online Supplementary Materials.

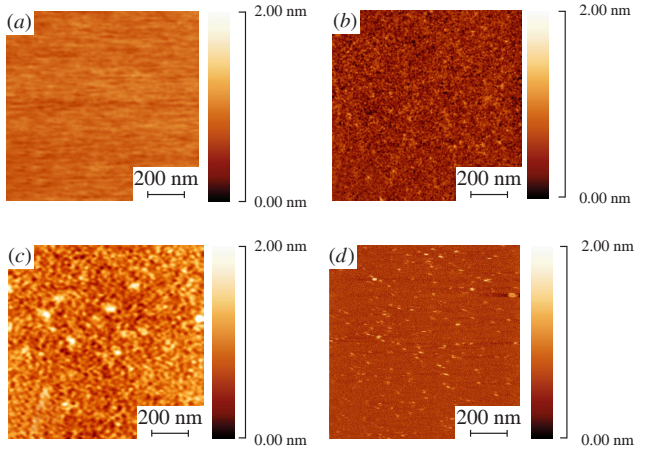

Figure 2 AFM images of a planar lipid bilayer on a mica substrate: (*a*) without additives, (*b*) with adsorbed H-C_{60}-L-Ala-OK nanoparticles, (*c*) with adsorbed H-C_{60}-D-Ala-OK nanoparticles and (*d*) with H-C_{60}-L-Ala-OK added at the liposome preparation stage.

showing a two-fold difference between adjacent maxima in the radius distribution.

For the D-alanine derivative (H-C_{60}-D-Ala-OK), the particle size measured by AFM in water ranges from 5.0 to 15.0 nm, with the majority of particles corresponding to a size of 9.0 ± 3.0 nm.

To investigate the ability of AAFDs to penetrate into the lipid bilayer, supported lipid bilayers consisting of 1,2-dioleoylphosphatidylcholine, 1,2-dioleoylphosphatidylserine, 1,2-dioleoylphosphatidylethanolamine and cholesterol were used. When liposomes prepared in a buffer solution were placed on a mica support, a lipid bilayer of about 4 nm thickness was formed.[12]

The experiments were conducted in two configurations: (1) deposition of AAFDs on the surface of the supported lipid bilayer and (2) mixing of the studied compounds in liposomes during their preparation (Figure 2).

In the first case, the height of the nanoparticles protruding above the surface of the lipid bilayer and in contact with the aqueous phase ranged from 1 to 3 nm. Given that the bilayer thickness is 4 nm, it is likely that nanoparticles with a diameter larger than the bilayer thickness were visible above the surface of the lipid bilayer, while those with a diameter of less than 4 nm were completely immersed in the bilayer. A similar result was observed when introducing AAFD at the stage of liposome preparation.

Since the localization of the studied compounds inside lipid membranes could affect their structural and dynamic parameters, an additional investigation of their physicochemical properties was carried out using the fluorescent probe method.† When pyrene was added to the erythrocyte suspension containing H-C_{60}-D-Ala-OK, effective quenching of pyrene fluorescence was observed compared to the control experiment (Figure 3). Additionally, changes were noted in the ratio between excimer fluorescence (λ_{em} = 454 nm)

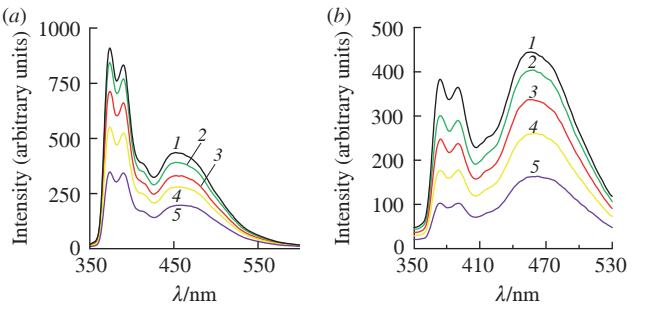

Figure 3 Fluorescence spectrum of 5 μM pyrene in an erythrocyte suspension at (*a*) λ_{exc} = 337 nm and (*b*) λ_{exc} = 280 nm (*1*) in the absence of additives (control) and in the presence of (*2*) 10, (*3*) 25, (*4*) 50 and (*5*) 100 μM H-C_{60}-D-Ala-OK.

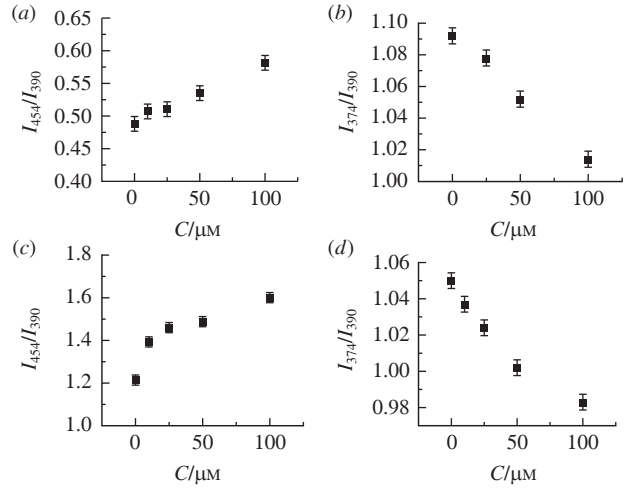

Figure 4 Dependence of (*a*) the microviscosity of the lipid bilayer, (*b*) the polarity of the microenvironment of pyrene monomers in total lipids, (*c*) the microviscosity of protein–lipid contacts and (*d*) the polarity of the microenvironment of pyrene monomers in annular lipids of human blood erythrocyte membranes on the concentration of introduced H-C_{60}-D-Ala-OK, determined by the fluorescent probe method.[13]

and monomer fluorescence (λ_{em} = 390 nm), as well as in the ratio between the maxima in the fluorescence band of pyrene monomers (Figure 4).

The dependence of the physicochemical parameters of biological membranes of human blood erythrocytes on the concentration of introduced H-C_{60}-D-Ala-OK was determined using the fluorescent probe method. The excimerization coefficient (the ratio of the fluorescence intensity of pyrene excimers at 454 nm to that of its monomers at 390 nm, I_{454}/I_{390}) at λ_{exc} = 337 nm reflects the change in the microviscosity of the lipid bilayer [Figure 4(*a*)]. The ratio of the fluorescence intensities at wavelengths of 374 and 390 nm (I_{374}/I_{390}) at λ_{exc} = 337 nm demonstrates a change in the polarity of the microenvironment of pyrene monomers in total lipids [Figure 4(*b*)]. The excimerization coefficient at λ_{exc} = 280 nm characterizes the change in the microviscosity of protein–lipid contacts [Figure 4(*c*)]. The I_{374}/I_{390} ratio at λ_{exc} = 280 nm indicates changes in the polarity of the microenvironment of pyrene monomers in annular lipids [Figure 4(*d*)].[13]

The quenching of pyrene fluorescence compared to the control in all experiments indicated an effective interaction of the fullerene derivative with excited pyrene molecules in both monomeric and excimer forms. The increase in the excimer to monomer pyrene fluorescence ratio upon addition of AAFD to erythrocytes demonstrated a statistically significant decrease in membrane microviscosity affecting both lipid–lipid and protein–lipid interactions (Table 1).

A decrease in the ratio of fluorescence intensities of pyrene monomers at wavelengths of 374 and 390 nm indicated an increase in the polarity of the microenvironment of the fluorescent probe molecules[13] upon the introduction of the fullerene derivatives. In the presence of both pyrene and fullerene in the same medium but without erythrocytes, the fluorescence intensity of pyrene monomers

Table 1 Structural and dynamic parameters of human blood erythrocyte membranes depending on the added fullerene derivative.

Sample	$I_{excimer}/I_{monomer}$ (λ_{exc}/nm)		I_{374}/I_{390} (λ_{exc}/nm)	
	337	280	337	280
Without additive (control)	0.488	1.214	1.092	1.050
H-C_{60}-D-Ala-OK (25 μM)	0.511	1.460	1.078	1.024
H-C_{60}-L-Ala-OK (25 μM)	0.522	1.450	1.018	0.988

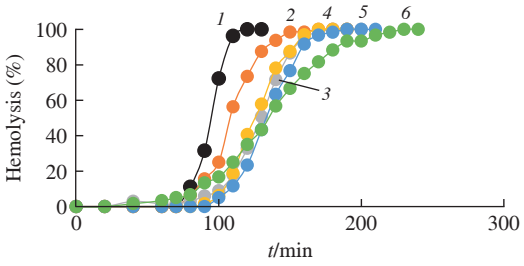

Figure 5 AAPH-induced hemolysis of human blood erythrocyte suspension (*1*) in the absence (control) and presence of H-C_{60}-L-Ala-OK at concentrations of (*2*) 1, (*3*) 10 and (*4*) 100 nM, as well as (*5*) 1 and (*6*) 10 μM.

at 390 nm was higher than at 374 nm, which is typical for an aqueous medium. The introduction of a fullerene derivative into a medium without erythrocytes led to a decrease in the ratio of pyrene excimers to monomers, whereas in a suspension of erythrocytes, excimerization increased upon the addition of a fullerene derivative.

The increase in the polarity of the microenvironment in the regions of lipid–lipid and lipid–protein interactions may be due to the presence of polar groups of the fullerene derivatives incorporated into the lipid bilayer, as well as a potential increase in membrane hydration. These factors may contribute to the observed decrease in microviscosity. Within the studied concentration range from 10 to 100 μM, the effects are monotonic and dose-dependent (see Figure 4).

The results suggest that the studied compounds either accumulate in membranes or are capable of passing through them. By increasing membrane fluidity, AAFDs can enhance the rate of biochemical processes in membranes. This effect, for example, could inhibit the generation of ROS in the inner mitochondrial membranes.

Previously, our studies demonstrated the protective effect of AAFDs in a model chemical system of liquid-phase radical oxidation of phosphatidylcholine liposomes.[14] In this work, we investigated their protective activity in a biological model system of free radical oxidation using human blood erythrocytes (Figure 5).[†]

The obtained results indicate that AAFDs exhibit a membrane-protective effect against damage to erythrocyte membranes caused by alkylperoxy radicals generated during thermal decomposition of AAPH. This effect is manifested at very low, nanomolar concentrations and reaches a plateau at higher concentrations.

Our work has shown that AAFDs, in particular with L- and D-alanine isomers, in the form of nanoparticles are effectively integrated into the lipid bilayers of biological membranes, reducing their microviscosity and increasing fluidity. Using the fluorescent probe pyrene, an increase in the polarity of the membrane microenvironment was observed upon the addition of the fullerene derivatives, which correlates with their membranotropic activity. Experiments with oxidative hemolysis of erythrocytes induced by AAPH confirmed the dose-dependent protective effect of the studied compounds, emphasizing their potential to suppress free radical processes. The protective effect against oxidative stress in erythrocyte membranes, observed even at a reduced concentration of AAFD (10^{-9} M), confirms the previously described ability of these compounds to exhibit biological activity at low doses in various agricultural applications.[15]

Based on the obtained data, it can be concluded that the membrane protection mechanism is associated not only with direct neutralization of radicals, but also with modulation of the structural and dynamic properties of the lipid bilayer. A decrease in membrane microviscosity may reduce the probability of electron leakage in mitochondria, thereby preventing the generation of ROS. Together with our previous studies,[14] these results provide a physicochemical basis for the application of water-soluble amino acid derivatives of fullerene C_{60} in biotechnology and agriculture.

This work was partially supported by the Ministry of Science and Higher Education of the Russian Federation (project nos. 125012000470-01 and 1022041900055-1-1.4.3;1.6.7 44.4.). We thank Margarita A. Gradova, PhD, Senior Researcher at FRCCP RAS, for her assistance with fluorescence measurements.

Online Supplementary Materials

Supplementary data associated with this article can be found in the online version at doi: 10.71267/mencom.7774.

References

1 V. S. Sokolov, O. V. Batishchev, S. A. Akimov, T. R. Galimzyanov, A. N. Konstantinova, E. Malingriaux, Y. G. Gorbunova, D. G. Knyazev and P. Pohl, *Sci. Rep.*, 2018, **8**, 14000; https://doi.org/10.1038/s41598-018-31901-9.

2 O. V. Batishchev, M. A. Kalutskii, E. A. Varlamova, A. N. Konstantinova, K. I. Makrinsky, Y. A. Ermakov, I. N. Meshkov, V. S. Sokolov and Y. G. Gorbunova, *Front. Mol. Biosci.*, 2023, **10**, 1192794; https://doi.org/10.3389/fmolb.2023.1192794.

3 F. Beuerle, R. Lebovitz and A. Hirsch, in *Medicinal Chemistry and Pharmacological Potential of Fullerenes and Carbon Nanotubes*, eds. F. Cataldo and T. Da Ros, Springer, Dordrecht, 2008, pp. 51–78; https://doi.org/10.1007/978-1-4020-6845-4_3.

4 Y. Chi, J. B. Bhonsle, T. Canteenwala, J.-P. Huang, J. Shiea, B.-J. Chen and L. Y. Chiang, *Chem. Lett.*, 1998, **27**, 465; https://doi.org/10.1246/cl.1998.465.

5 Z. Wang, S. Wang, Z. Lu and X. Gao, *J. Cluster Sci.*, 2015, **26**, 375; https://doi.org/10.1007/s10876-015-0855-0.

6 S. M. Mirkov, A. N. Djordjevic, N. L. Andric, S. A. Andric, T. S. Kostic, G. M. Bogdanovic, M. B. Vojinovic-Miloradov and R. Z. Kovacevic, *Nitric Oxide*, 2004, **11**, 201; https://doi.org/10.1016/j.niox.2004.08.003.

7 R. V. Bensasson, M. Brettreich, J. Frederiksen, H. Göttinger, A. Hirsch, E. J. Land, S. Leach, D. J. McGarvey and H. Schönberger, *Free Radical Biol. Med.*, 2000, **29**, 26; https://doi.org/10.1016/S0891-5849(00)00287-2.

8 T. Baati, F. Bourasset, N. Gharbi, L. Njim, M. Abderrabba, A. Kerkeni, H. Szwarc and F. Moussa, *Biomaterials*, 2012, **33**, 4936; https://doi.org/10.1016/j.biomaterials.2012.03.036.

9 J. Grebowski, P. Kazmierska, G. Litwinienko, A. Lankoff, M. Wolszczak and A. Krokosz, *Biochim. Biophys. Acta, Biomembr.*, 2018, **1860**, 1528; https://doi.org/10.1016/j.bbamem.2018.05.005.

10 R. A. Kotel'nikova, I. I. Faingol'd, D. A. Poletaeva, D. V. Mishchenko, V. S. Romanova, V. N. Shtol'ko, G. N. Bogdanov, A. Yu. Rybkin, E. S. Frog, A. V. Smolina, A. A. Kushch, N. E. Fedorova and A. I. Kotel'nikov, *Russ. Chem. Bull.*, 2011, **60**, 1172; https://doi.org/10.1007/s11172-011-0184-x.

11 M. V. Voronkov, V. A. Volkov, V. V. Volkov, V. S. Romanova, I. G. Plashchina and E. V. Sidorsky, *Mendeleev Commun.*, 2023, **33**, 823; https://doi.org/10.1016/j.mencom.2023.10.028.

12 M. V. Volovik, Z. G. Denieva, P. K. Gifer, M. A. Rakitina and O. V. Batishchev, *Biomolecules*, 2024, **14**, 1061; https://doi.org/10.3390/biom14091061.

13 R. A. Kotelnikova, A. V. Smolina, A. V. Zhilenkov, Yu. V. Soldatova, I. I. Faingold, P. A. Troshin and A. I. Kotelnikov, *Russ. Chem. Bull.*, 2018, **67**, 366; https://doi.org/10.1007/s11172-018-2082-y.

14 V. A. Volkov, M. V. Voronkov, N. N. Sazhina, D. V. Kurilov, D. V. Vokhmyanina, O. V. Yamskova, Yu. Ts. Martirosyan, D. L. Atroshenko, L. Yu. Martirosyan and V. S. Romanova, *Kinet. Catal.*, 2021, **62**, 395; https://doi.org/10.1134/S0023158421030095.

15 M. Voronkov, O. Tsivileva, V. Volkov, V. Romanova and V. Misin, *Processes*, 2023, **11**, 1695; https://doi.org/10.3390/pr11061695.

Received: 25th March 2025; Com. 25/7774